ADVANCES IN ATMOSPHERIC SCIENCES, VOL. 34, FEBRUARY 2017, 235–245

• **Original Paper** •

Relationship between Lightning Activity and Tropospheric Nitrogen Dioxide and the Estimation of Lightning-produced Nitrogen Oxides over China

Fengxia GUO*[1], Xiaoyu JU[1,2], Min BAO[1], Ganyi LU[1], Zupei LIU[1], Yawen LI[1], and Yijun MU[1]

[1]*Key Laboratory of Meteorological Disaster, Ministry of Education/Joint International Research Laboratory of Climate and Environment Change/Collaborative Innovation Center on Forecast and Evaluation of Meteorological Disaster/Key Laboratory for Aerosol–Cloud–Precipitation of China Meteorological Administration, Nanjing University of Information Science and Technology, Nanjing* 210044*, China*

[2]*Anhui Meteorological Disaster Prevention Center, Anhui 230061, China*

(Received 15 April 2016; revised 7 October 2016; accepted 9 October 2016)

ABSTRACT

To better understand the relationship between lightning activity and nitrogen oxides (NO_X) in the troposphere and to estimate lightning-produced NO_X (LNO_X) production in China more precisely, spatial and temporal distributions of vertical column densities of tropospheric nitrogen dioxide (NO_2 VCDs) and lightning activity were analyzed using satellite measurements. The results showed that the spatial distribution of lightning activity is greater in the east than in the west of China, as with NO_2 VCDs. However, the seasonal and annual variation between lightning and NO_2 density show different trends in the east and west. The central Tibetan Plateau is sparsely populated without modern industry, and NO_2 VCDs across the plateau are barely affected by anthropogenic sources. The plateau is an ideal area to study LNO_X. By analyzing 15 years of satellite data from that region, it was found that lightning density is in strong agreement with annual, spatial and seasonal variations of NO_2 VCDs, with a correlation coefficient of 0.79 from the linear fit. Combining Beirle's method and the linear fit equation, LNO_X production in the Chinese interior was determined to be 0.07 (0.02–0.27) TgN yr^{-1} for 1997–2012, within the range of 0.016–0.384 TgN yr^{-1} from previous estimates.

Key words: lightning, tropospheric NO_2, LNO_X

Citation: Guo, F. X., X. Y. Ju, M. Bao, G. Y. Lu, Z. P. Liu, Y. W. Li, and Y. J. Mu, 2017: Relationship between lightning activity and tropospheric nitrogen dioxide and the estimation of lightning-produced nitrogen oxides over China. *Adv. Atmos. Sci.*, **34**(2), 235–245, doi: 10.1007/s00376-016-6087-x.

1. Introduction

Nitrogen oxides ($NO_X = NO + NO_2$, where NO is nitric oxide and NO_2 is nitrogen dioxide), with maximum density in the odd nitrogen family, are the most important trace gases in tropospheric chemistry. Natural nitrogen (N) is continuously cycled by many different processes (Xu et al., 2012). Near the ground, NO_X, with a very short atmospheric lifetime (several hours), mainly originates from anthropogenic combustion (fossil fuel combustion and biomass burning) and biogenic soil emissions. These sources primarily influence the lower troposphere at local scale. The residence time of NO_X is increased in the upper troposphere (Levy et al., 1996). Some significant tropospheric sources of NO_X, such as lightning, stratospheric injection, ammonia oxidation and aircraft exhaust, directly affect the global troposphere (Schumann et al., 2000). However, the magnitudes of these sources are smaller than those of surface sources. Minor sources, such as emissions from mid- and long-range aircraft and the stratospheric injection of NO_X formed by photolysis of nitrous oxide and nitric acid (HNO_3), also strongly affect the photochemistry of the upper troposphere (Huntrieser et al., 1998).

NO_X is the most critical type of gases directly impacting photochemical ozone (O_3) and hydrocarbon production in the troposphere. During the circulation of NO_X, ozone are produced in places where it is highly concentrated, and carbon monoxide (CO), methane and other unstable organic components accelerate this process (Crutzen, 1970). Photochemical smog is also produced, which reduces visibility and harms human health. NO_X with lower density reduces ozone production rates (Seinfeld and Pandis, 2016). By oxidization of hydroxyl (OH), NO_X can convert to HNO_3, which, together with sulfuric acid (H_2SO_4) generated by sulfur dioxide (SO_2), directly contributes to rainwater acidity at regional levels. As a consequence, NO_X affects the density of tropospheric O_3 and OH and, therefore, partially control the level of oxidants.

NO_X is produced in the very hot lightning channel, owing to oxygen (O_2) and nitrogen (N_2) dissociation (Zel'dovich

* Corresponding author: Fengxia GUO
Email: guofx@nuist.edu.cn

and Raizer, 1967). When channels cool to 3000–4000 K, NO is formed in the plasma and is "frozen in" during the subsequent cooling. NO is converted to NO_2 by reaction with ambient O_3 and photolyzed back to NO during daytime. An equilibrium state is reached after about 100 s.

Although lightning-produced NO_X (LNO_X) accounts for only 10%–20% of global NO_X, lightning is responsible for at least 50% of the initial NO_X in the upper troposphere, and only 20% of NO_X originates from upward transport from the ground (Seinfeld and Pandis, 2016). More than 70% of NO_X is from lightning in the tropopause, especially in tropical and subtropical regions (Martin et al., 2002). In addition to conveying substantial NO_X in the troposphere, LNO_X affects the generation of tropospheric O_3. The production of O_3 caused by LNO_X is six times greater than that of anthropogenic NO_X emissions (Wu et al., 2007). Therefore, the distribution and change of LNO_X is important in global climate change (Qie et al., 2015). Moreover, lightning is sensitive to that change. LNO_X will increase 15% K^{-1} with a global temperature rise of 1.5–5.8 K and, as a consequence, the increase of LNO_X will feedback to climatic cycles (Williams, 2005).

With the gradual realization of the importance of lightning to the global N cycle, estimating the production of LNO_X has become a focus in the study of lightning. Several methods have been used to estimate NO production per flash. The earliest estimates came from theoretical considerations of the lightning energy dissipation rate and NO yield per joule, based on *in situ* measurements. More recently, estimates have come from laboratory spark measurements. Some of these experiments were conducted to collect NO_X produced by sparks (Wang et al., 1998; Cooray et al., 2009), and could assess the contribution from various lightning processes and parameters. Based on these, the global production of LNO_X can be extrapolated. Within such methods, in general, lightning parameters such as channel temperature, peak current, atmospheric pressure, and channel length are referred to as extrapolation parameters, and only the return stroke is considered. Other lightning processes are ignored.

Methods to estimate LNO_X production in recent studies have limitations. First, the peak current and energy of sparks produced in the laboratory are less than those of a natural lightning flash. Second, the environment inducing lightning flashes is difficult to replicate in the laboratory. Third, parameters involved in theoretical estimation and their corresponding values varied in the studies, resulting in great differences. Consequently, estimates of the global production of LNO_X are still highly uncertain, covering a wide range (2–20 TgN yr^{-1}) (Schumann and Huntrieser, 2007). Chinese studies have also produced a large range, from 0.016 to 0.384 TgN yr^{-1} (Zhou and Qie, 2002; Sun et al., 2004; Lin, 2012) (Table 1).

Compared with theoretical calculations of global LNO_X production based on laboratory simulation and *in situ* observation, estimates based on satellite measurements, which can provide several years of observation and global datasets, is a comprehensive method for detecting atmospheric trace gases. To avoid the other sources, Beirle et al. (2004) obtained a relationship between lightning and NO_2 VCDs (vertical column densities of tropospheric NO_2) in the central Australian desert, which has limited anthropogenic NO_X emissions, using Global Ozone Monitoring (GOME) satellite data, and then estimated a global LNO_X production of 2.8 (chosen from the range 0.8–14) TgN yr^{-1}. Several previous studies (Boersma et al., 2005; Martin et al., 2007; Miyazaki et al., 2014) have provided comprehensive constraints on estimates of the global LNO_X source by using satellite retrievals of NO_2 to constrain LNO_X sources and global chemical transport models. Boersma et al. (2005) presented a first attempt to estimate the global LNO_X production by comparing observed NO_X from the GOME satellite spectrometer with modeled LNO_X distributions simulated by the global chemical transport model TM3 including two lightning parameterizations: one based on convective precipitation, and one based on the fifth power of the cloud top height. They estimated the global LNO_X production to be in the range 1.1–6.4 TgN in 1997. Martin et al. (2007) used observations of trace gases from the Scanning Imaging Absorption Spectrometer for Atmospheric Chartography (SCIAMACHY), Ozone Monitoring Instrument (OMI) and Microwave Limb Sounder, and Atmospheric Chemistry Experiment Fourier Transform Spectrometer satellite platforms to provide top-down constraints on the production of NO by lightning. A global chemical transport model (GEOS-Chem) was used to identify locations and time periods in which lightning would be expected to dominate the trace-gas observations. A global source of 6 ± 2 TgN yr^{-1}

Table 1. Overview of recently published estimates of annual lightning NO_X production in China. *P* denotes the estimated production of LNO_X.

Study	*P* (units: TgN yr^{-1})	Range (units: TgN yr^{-1})	Location	Method
Zhou and Qie (2002)	0.384	–	China	Extrapolation of CG flashes location data
Sun et al. (2004)	0.016	–	China	Extrapolation of satellite total lightning data
Lin (2012)	0.21	0.08–0.34	East China	Regression-based multi-step inversion approach based on NO_2 VCDs retrieved from the OMI and GEOS-Chem model
This study	0.07	0.02–0.27	China	Extrapolation of satellite total lightning data

from lightning in the model best represented the satellite observations. These approaches have the potential to reduce the influence of model errors in, and thus improve the estimation of, LNO_X source estimation, by simultaneously optimizing various aspects of the chemical system.

Lin (2012) presented a regression-based multi-step inversion approach to separately estimate emissions of NO_X from anthropogenic, lightning and soil sources, for the year 2006 over East China, based on NO_2 VCDs retrieved from the OMI and GEOS-Chem model. The inversion estimate suggested annual budgets of about 7.1 TgN (±39%), 0.21 TgN (±61%), and 0.38 TgN (±65%) for the *a posteriori* anthropogenic, lightning and soil emissions, respectively, which were about 18%–23% higher than the respective *a priori* values. Recently, Miyazaki et al. (2014) estimated the global source of LNO_X by assimilating observations of NO_2, O_3, HNO_3 and CO measured by multiple satellite measurements into a chemical transport model. The annual global LNO_X source amount and NO production efficiency were estimated at 6.3 TgN yr^{-1}.

In the present work, we examined 15 years (1997–2012) of satellite lightning data and NO_2 VCDs over China. We found that the Tibetan Plateau is an ideal region to research the correlation between these two variables. Thus, based on their correlation over the Tibetan Plateau, we extrapolated LNO_X production to the whole of China.

2. Data

2.1. *Lightning*

The lightning data in this paper were selected from the latest (version 2.3) Optical Transient Detection/Lightning Imaging Sensor (OTD/LIS) gridded dataset from the Global Hydrology Resource Center. There were five years of OTD data (April 1995 through March 2000) and 14 years of LIS data (January 1998 through February 2012). The full data period was 17 years. The two detectors observe total lightning flashes and do not distinguish cloud from ground discharges (Cecil et al., 2014).

The OTD is carried aboard the MicroLab-1 satellite that was launched in April 1995. The orbit is approximately circular. The altitude of MicroLab-1 is 740 km, with an inclination of 70° and observation window of 1300 km × 1300 km. Its spatial resolution is 10 km and temporal resolution 2 ms. The sensors use narrowband optical filtering to select an oxygen triplet line generated by atmospheric lightning centered at 777.4 nm. The OTD detection efficiency was ~48% in 1996 (Boccippio et al., 2000). LIS is carried on the Tropical Rainfall Measure Mission platform, launched in 1997. The sensor detects and locates rapid changes in the brightness of clouds as they are illuminated by lightning discharges, providing information on the time, location, radiation and duration of total lightning flashes. The latitude range was initially ±35°, which increased to ±39° after the satellite was boosted from 350 to 402 km altitude.

2.2. *Tropospheric NO_2 column*

The study exploits information on VCDs of tropospheric NO_2 for all years between 1997 and 2012, retrieved from the GOME, SCIAMACHY and the second generation of Global Ozone Monitoring (GOME-2) measurements by KNMI (the TM4NO2A product, version 2.3: monthly mean).

GOME is carried on the ERS-2 satellite, launched on 21 April 1995, with a sun-synchronous, near-polar orbit. It consists of four spectrometers measuring radiation reflected by Earth in the UV/visible spectral range (240–790 nm), with a resolution of 0.2–0.4 nm. GOME measures the distributions of trace gases such as O_3 and NO_2. Through advanced microwave remote sensing technology, GOME can acquire images continuously, which is superior to traditional means. Based on several years of GOME operation, GOME-2 has been developed. It was installed aboard the METOP-A satellite and launched in October 2006. GOME-2 has an improved design. The compatibility of high radio frequency enhanced the sensitivity of the microwave detection unit. The minimum detectable signal was reduced to 70 dB. The polarization detection ability and correction technology were greatly improved. SCIAMACHY was developed from GOME, and can observe trace gases throughout the atmosphere via a detection method of nadir, limb and occultation. It was carried by an ENVISAT polar-orbiting satellite launched in March 2002 to an altitude of 800 km, with an inclination of 98°. The spatial resolution of SCIAMACHY is 60 km × 30 km, and covers the globe in 6 days.

The monthly tropospheric NO_2 column products used herein are residuals from subtracting two large numbers (total slant column and stratospheric slant NO_2 column) that are both subject to noise. The products were then reanalyzed and corrected by the TM3 chemical model, converting them into gridded data (Boersma et al., 2004). There are already many mature research results regarding the algorithm, retrieval method, ground validation, and error analysis of NO_2 VCDs. We chose the period from February 1997 to February 2012. However, given the different observing instruments, data from February 1997 through December 2003 were observed by GOME, January 2004 through December 2006 by SCIAMACHY, and January 2007 through February 2012 by GOME-2. We calculated average data of the other 14 months of January to fill in missing data of NO_2 VCDs in January 1998.

The column amount of NO_2 has been retrieved using the Differential Optical Absorption Spectroscopy technique. If a significant tropospheric slant column density is retrieved, a meaningful estimate of the tropospheric vertical column can be given with a precision of 35%–60%. These retrieval uncertainties are associated with the computation of the tropospheric air mass factor. The most important uncertainties associated with the computation of the tropospheric air mass factor are cloud fraction, surface albedo and profile shape (Boersma et al., 2004). The transit time of GOME and GOME-2 and SCIAMACHY is between 0930 and 1030 LST (local standard time). Richter et al. (2005) showed excellent consistency among processed data from these three platforms, using the same retrieval method.

3. Distribution of lightning flashes and tropospheric NO_2 columns

3.1. *Lightning flashes*

Figure 1 shows that the regional distributions of lightning densities varied greatly over China. The most intense lightning activity was focused offshore, with moderately intense activity over the central region and weak activity over western China. The average lightning density was 10.4 flashes km^{-2} yr^{-1} in eastern China and less than 10.4 flashes km^{-2} yr^{-1} in the central region. The maximum density, along the Yunnan–Guizhou Plateau to Guangzhou area, was 18.9–29.8 flashes km^{-2} yr^{-1}. There was low lightning frequency (an average of less than 1 flash km^{-2} yr^{-1}) in western interior regions such as the Xinjiang and Tibet borders, because they are distant from the ocean and dominated by an arid climate. Thus, they have little rain throughout the year and weak thunderstorm activity (Lin and Wu, 1981). Lightning activity on the north and south sides of the Himalaya showed a great difference. Compared with adjacent areas in the western region, lightning was more frequent, with a density of 6.2–8.4 flashes km^{-2} yr^{-1} over the Tibetan Plateau. There was a clear difference in lightning between land and sea in China. Coastal areas, such as Guangxi, Guangdong, Fujian, Taiwan and Hainan, were centers of high lightning density. Regional differences were similar to Yuan and Qie (2004).

Figure 2 shows an obvious monthly variation of lightning. Lightning flashes begin to increase after January, maximizing in July and August. There is a dramatic decrease from September, with minima in November, December and January. The highest lightning frequency in China is in summer (June through August), accounting for about 70% of total lightning flashes. Spring (March through May) accounts for ~20%, followed by autumn (September through November). The minimum is in winter (December through February), with a frequency smaller than that of summer by an order of magnitude.

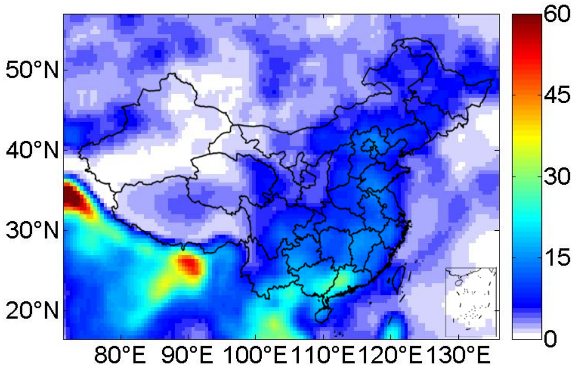

Fig. 1. Spatial distribution of annual average lightning density in the region (16°–56°N, 71°–136°E) during February 1997 to February 2012, based on 0.5 Degree High Resolution Full Climatology (HRFC) data of OTD/LIS (units: flashes km^{-2} yr^{-1}).

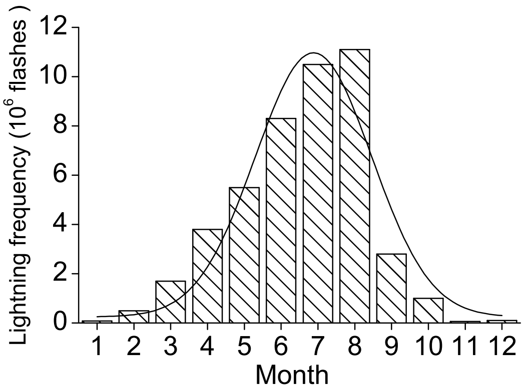

Fig. 2. Monthly variation of average lightning flashes in China during February 1997 to February 2012, based on 2.5 Degree Low Resolution Full Climatology (LRFC) data of OTD/LIS. Solid line is the fitting curve.

3.2. *Tropospheric NO_2 columns*

Figure 3 shows that tropospheric NO_2 VCDs were mainly in three areas: North China and the Yangtze and Pearl River deltas, which are densely populated areas with intensive industry and agriculture (National Bureau of Statistics of China, 2012). This indicates that human activities significantly affect tropospheric NO_2 VCDs. Tropospheric NO_2 density around the Tibetan Plateau is higher than surrounding areas. The plateau has little industrial production and is sparsely populated (National Bureau of Statistics of China, 2012). As a consequence, its anthropogenic NO_X emissions are limited (Shi et al., 2014). However, its geographic location and climate cause it to have greater thermal convection (Qian et al., 2001), so the contribution of LNO_X to total NO_X is large. There is a high NO_2 density around Ürümqi, at the center of northern Xinjiang. Lightning activity is at a minimum there (Fig. 1), but the area has a larger population and more developed economy than those of surrounding areas (National Bureau of Statistics of China, 2012). This again shows that human activity has a significant effect on tropospheric NO_2.

Using the GEOS-Chem model, Lin (2012) also found that anthropogenic emissions are the dominant sources of NO_X over the whole of China. Rapid economic development promotes increases in industrial burning and vehicle exhaust, especially in densely populated areas such as eastern China where the composition of tropospheric NO_X sources is more complex. In contrast, anthropogenic emissions of NO_X from the Tibetan Plateau, with its lower industrial production, are limited, and the major tropospheric NO_X is natural in origin.

Two regions at the same latitude (30°–38°N) but variable longitude (110°–122°E, 80°–92°E), representing the eastern and western parts of China, respectively, were selected to analyze their monthly variations of tropospheric NO_2 VCDs. As shown in Fig. 3, region a, (eastern China) mainly includes Shandong, Anhui, Jiangsu, Henan and Hubei.

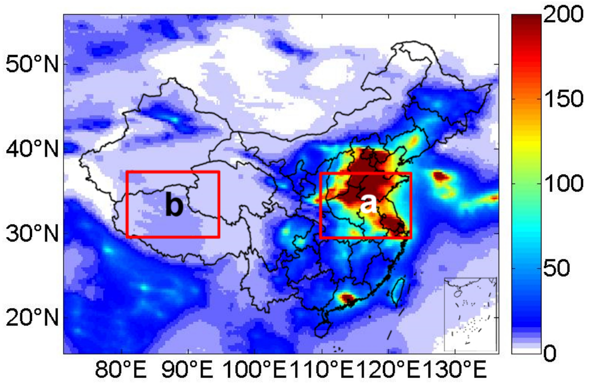

Fig. 3. Distribution of average tropospheric NO_2 VCDs in the region (16°–56°N, 71°–136°E) during February 1997 to February 2012, based on GOME-1/2 and SCIMACHY data [Region a: (30°–38°N, 110°–124°E); Region b: (30°–38°N, 80°–94°E); units: 10^{14} molecules cm^{-2}].

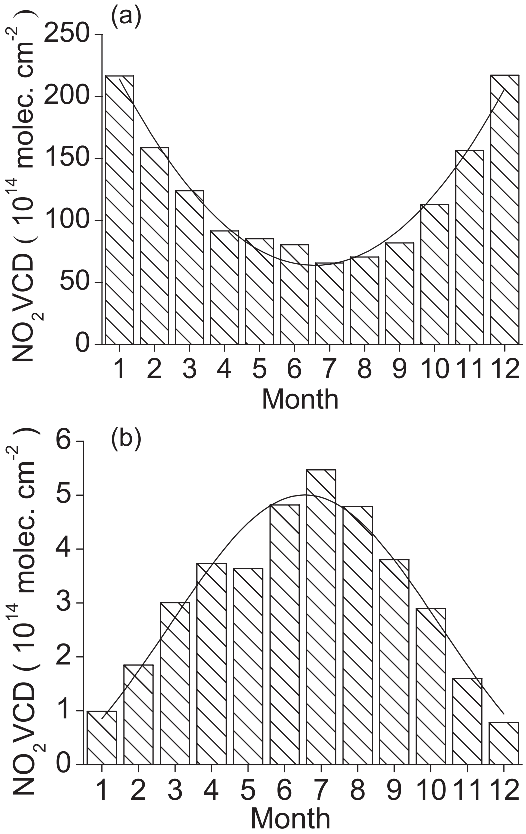

Fig. 4. Monthly variation of average tropospheric NO_2 VCDs in (a) eastern (30°–38°N, 110°–124°E) and (b) western (30°–38°N, 80°–94°E) China during February 1997 to February 2012, based on GOME-1/2 and SCIMACHY data. Solid line is the fitting curve.

Region b (western China), mainly includes northwestern Tibet, southern Xinjiang and western Qinghai.

The tropospheric NO_2 VCDs present opposite trends with season between the eastern and western areas (Fig. 4). The maximum NO_2 density was in winter and the minimum in summer in eastern China, and the reverse in western China. Tropospheric NO_2 VCDs in the east were an order of magnitude greater than those in the west during summer and two orders of magnitude in winter. Although anthropogenic emissions did not have clear seasonal variation, convection is weak and unfavorable for atmospheric diffusion in winter, so the emissions of NO_2 persist for a long time in the troposphere. Figures 2 and 4 show that the monthly variation of tropospheric NO_2 VCDs in eastern China was nearly opposite to the variation of lightning flashes across China, but similar to lightning in western China.

3.3. *Correlation between lightning and tropospheric NO_2 columns in eastern and western China*

Figure 5 shows that monthly variations of average lightning density over 15 years in the eastern and western regions were consistent. Seasonal change showed low densities in winter and high densities in summer. Overall, yearly peak lightning frequency in the eastern region was several times greater than that in the west. Among the 15 years, maximum lightning frequency was during July 2006 in the east, and July 2002 in the west. Monthly variations of tropospheric NO_2 VCDs revealed markedly different trends across the east and west, similar to Fig. 4. This indicates that tropospheric NO_2 VCDs in the east are strongly affected by human activities, and the contribution from lightning is very slight. Moreover, it suggests that the sparse population and low level of industrial production in the west cause lightning to be the major source of tropospheric NO_2 there, although lightning flashes were less frequent than in the east.

Zhang et al. (2007) studied the trend of tropospheric NO_2 VCDs in China from 1997 to 2007. They also showed the maximum tropospheric NO_2 density during winter in eastern China, which was mainly attributed to anthropogenic emissions. The maximum density was during summer in western China, mainly produced by natural emissions.

The tropospheric NO_2 VCDs generally had an increasing trend (especially in recent years), with an average annual growth rate of 4.5% in eastern China. Trends of lightning activity and tropospheric NO_2 VCDs were in strong agreement in western China, and the latter were lower by one or two orders of magnitude relative to eastern China. In the west, the annual peak NO_2 density was very stable, with no obvious difference over the 15 years. Xiao et al. (2011) used OMI satellite remote sensing data to study atmospheric NO_2 in China. They indicated an increase of tropospheric NO_2 VCDs in the Yangtze River Delta and other eastern regions. However, over the Tibetan Plateau and in other western regions, there was a stable interannual variability with the maximum frequently in summer.

Lightning and soil emissions have similar seasonality. Yienger and Levy (1995) included soil emissions due to microbiological processes producing NO_X naturally, as well as those associated with the use of chemical fertilizers and manure. Soil emissions of NO_X over China are of great interest because of the extensive use of fertilizers (Lin, 2012). Region

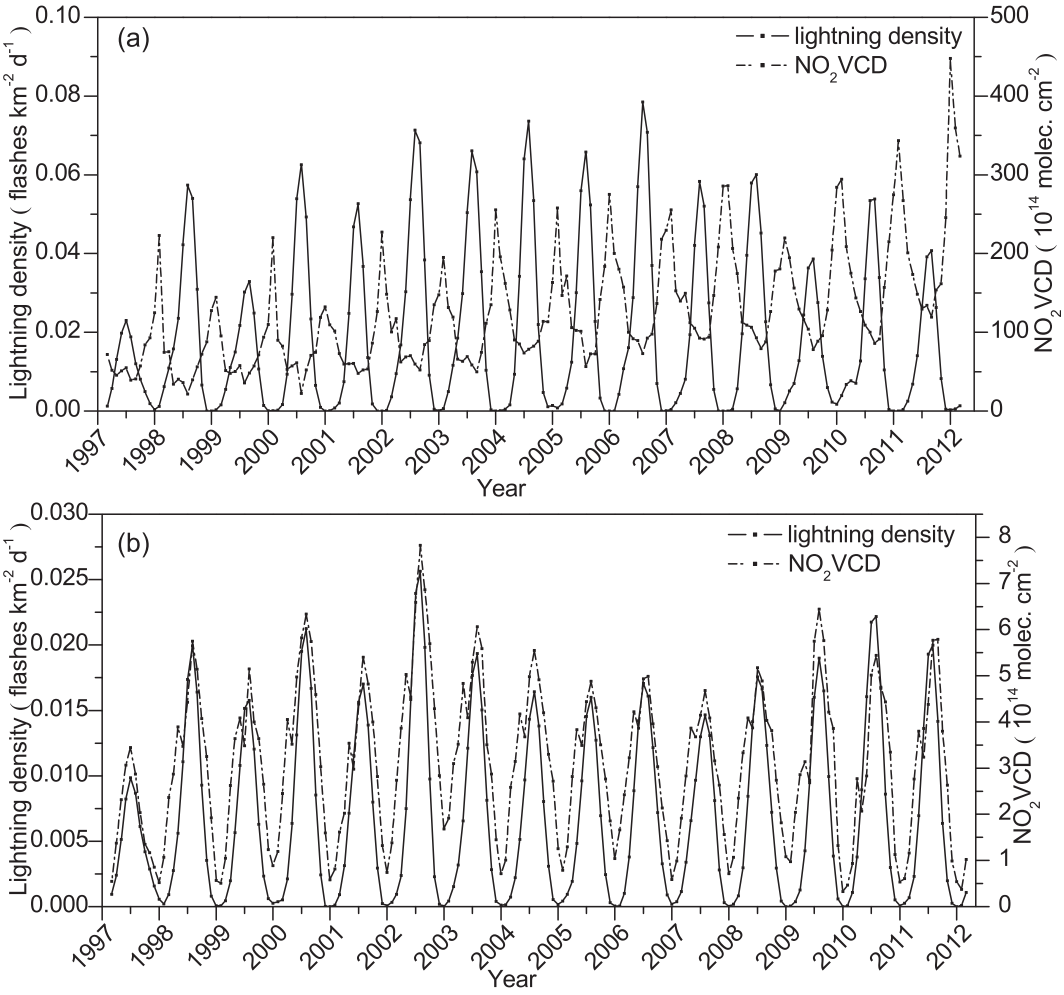

Fig. 5. Monthly variation of average lightning density and tropospheric NO_2 VCDs in (a) eastern (30°–38°N, 110°–124°E) and (b) western (30°–38°N, 80°–94°E) China during February 1997 to February 2012, based on LRFC data of OTD/LIS and GOME-1/2 and SCIMACHY data, respectively.

b mainly includes northwestern Tibet, western Qinghai and southern Xinjiang. Northwestern Tibet and western Qinghai are located in the plateau hinterland, controlled by a continental cold and dry climate. Tarim Basin, located in southern Xinjiang, is very arid and controlled by a temperate desert climate. Taklimakan Desert is inside the Tarim Basin. Region b is barren or sparsely vegetated, and mainly covered with grassland and open shrubland, so fertilizers are not used extensively. Vinken et al. (2014) also showed that Region b selected in this paper features only small quantities of soil emissions. In addition, interannual peaks of NO_2 VCDs and lightning match very well. So, it can be considered that soil emissions in Region b are very limited compared with lightning emissions.

All these findings indicate that lightning-produced NO_2 is the main source of tropospheric NO_2 in western China, and that tropospheric NO_X is mainly produced by anthropogenic emissions in the eastern region, although lightning flashes there are more numerous than in the west.

The contribution of lightning to NO_X is difficult to identify in areas with strongly anthropogenic NO_X sources and soil emissions. From the above discussion, we can conclude that the sparsely populated Tibetan Plateau, with its minimal industrial production, strong thermal convection and limited use of fertilizers, is an ideal region to investigate the relationship between lightning and tropospheric NO_X.

4. Correlation between lightning and tropospheric NO_2 columns of the Tibetan Plateau

Figure 6 shows the seasonal variation of lightning and NO_2 VCDs from 15 years of satellite observation data. Over this long period, the seasonal order of both maximum NO_2 VCDs and lightning flashes was summer, spring, autumn, and then winter. It can be seen that their summer variations were highly consistent every year, with both maximizing in 2002 and minimizing in 1997. In other seasons, lightning flashes seldom occurred, especially in winter, meaning other sources such as soil emissions and long-range transport were probably significant, in spite of relatively low magnitudes. As a consequence, the tendencies of NO_2 VCDs were generally

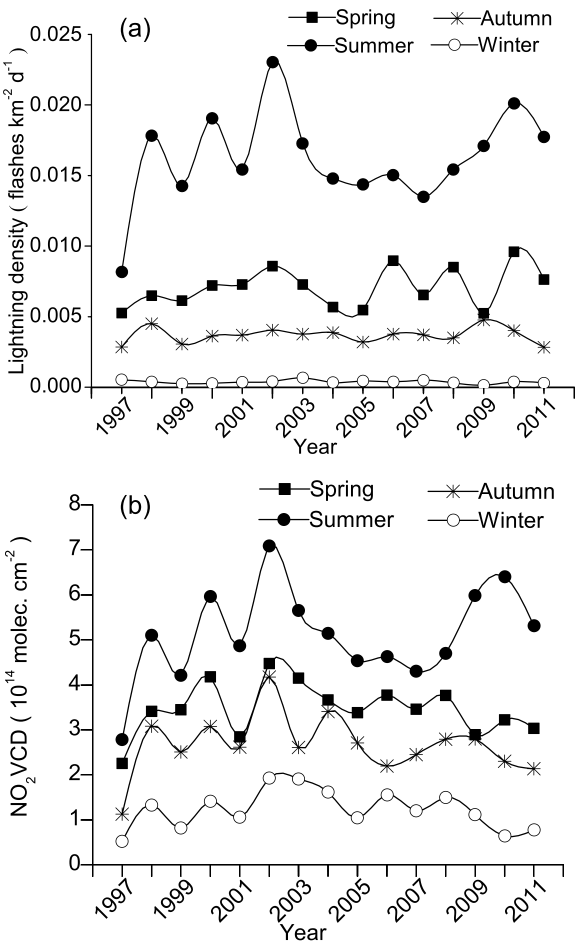

Fig. 6. Long-term seasonal trends of (a) lightning density and (b) tropospheric NO_2 VCDs across the central Tibetan Plateau (26°–37°N, 78°-100°E) during 1997–2012, based on LRFC data of OTD/LIS and GOME-1/2 and SCIMACHY data, respectively.

consistent with lightning in spring, autumn and winter, but the correlations were not as good as those in summer.

The above findings confirm that tropospheric NO_2 VCDs in the plateau region are barely influenced by human sources. In addition, there is almost no lightning in winter, but NO_2 is greater than zero, with a small and stable average value. This means that soil emissions and the photochemical release of ice may be the principal natural sources aside from lightning (Kang and Cong, 2006; Wang et al., 2011). Another possible cause is the horizontal transport of NO_2 over long distances from other places in winter, because of the relatively long chemical lifetime. The lifetime of NO_X has a significant relationship with temperature, i.e., the lower the temperature, the longer the lifetime. Zhang et al. (2007) studied the tendency of tropospheric NO_2 VCDs in China from 1997 to 2007. They stated that, in eastern China during winter, lightning was rare but the NO_2 VCDs remained greater than 8×10^{15} molecules cm^{-2} and had an average annual growth rate of 1.15×10^{15} flashes km^{-2} yr^{-1}; the contribution of lightning to NO_2 VCDs was very small. Consequently, eastern China is not appropriate for LNO_X research.

Figure 7 shows the linear-fit correlation between tropospheric NO_2 VCDs and lightning flashes summertime data only for the 15 years over the central Tibetan Plateau. The correlation coefficient reached 0.79. This confirms that the plateau is an ideal region to research the relationship between lightning and NO_X. The resulting slope is 221.99. These indicate the increase of tropospheric NO_2 caused by lightning flashes, based on satellite measurements. The error is 25.71 (units: 10^{24} molecules flashes^{-1} d^{-1}). The intercept of regression is 1.44. This reflects the background NO_2, attributed mainly to sources other than lightning. The intercepts in Fig. 7 are small compared to the range of values found. This shows that the method is efficient in reducing the influence of other sources, enhancing the significance of the regressions.

5. Estimation of LNO_X production in China

There have not been many studies of LNO_X in China. Zhou and Qie (2002) used observed lightning data at different latitudes and longitudes combined with physics theory to estimate LNO_X production in China at 0.384 TgN yr^{-1}. The data covered only Guangdong, Gansu, Beijing and northeastern China, so might have some limitations and specificity. Based on OTD data and theoretical calculation, Sun et al. (2004) attained 0.2 TgN yr^{-1} for the global average annual production of lightning-produced N, and 0.016 TgN yr^{-1} for China (7.8% of the global production). The aforementioned LNO_X estimates lack NO_X observation data. Satellite platforms can simultaneously and directly detect change of tropospheric NO_2 VCDs and lightning flashes, avoiding the complexity of physical parameter selection in theoretical calculation and extrapolation.

Over the Tibetan Plateau, tropospheric NO_X mainly originates from natural emissions, and NO_X contributions to such

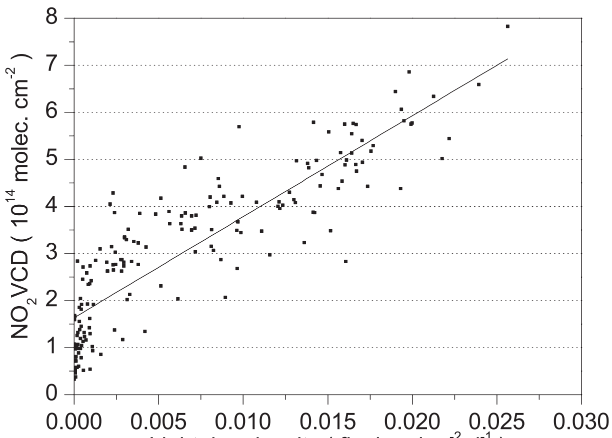

Fig. 7. Linear fit of monthly average lightning density and NO_2 VCDs over the central Tibetan Plateau (26°–37°N, 78°–100°E) during February 1997 to February 2012, based on LRFC data of OTD/LIS and GOME-1/2 and SCIMACHY data, respectively.

emissions other than from lightning are very slight. The positive correlation between tropospheric NO_2 VCDs and lightning flashes is clear. Therefore, based on this correlation for the Tibetan Plateau, estimation of nationwide LNO_X production in China can further reduce the influence of other sources. Based on the method proposed by Beirle et al. (2004), we made a rough estimate of LNO_X production in China.

First, the daily NO_X emission amount was obtained via

$$P_{\rm day} = \frac{F\,{\rm VCD}_{\rm NO_2}}{\tau f_{\rm NO_2}} , \tag{1}$$

where F is a correction factor. Because tropospheric trace gases depend on the vertical profile, surface albedo and cloud cover, the retrieved NO_2 VCDs must be corrected. The correction factor for NO_2 in the boundary layer is generally ∼4, but may be close to 1 in cloud-free deserts. Cloud cover over the central Tibetan Plateau is less and the visibility of satellite observations is high, so we selected 1.5 (1–2).

$f_{\rm NO_2}$ is the ratio of NO_2 to NO_X in the troposphere:

$$f_{\rm NO_2} = \frac{\rm NO_2}{\rm NO_X} . \tag{2}$$

$f_{\rm NO_2} = 0.6$ (0.4–0.8) in this paper, as per the result of the Pollution from Aircraft Emissions in the North Atlantic Flight Corridor 2 project (Ziereis et al., 2000). It was found that the ratio increased with latitude at the top of the troposphere and lower stratosphere, around 28°–61°N in the Northern Hemisphere.

The lifetime τ of NO_2 controls the accumulation of NO_2 in the atmosphere, and NO_2 VCDs are proportional to τ for a constant source. For the Tibetan Plateau, we selected 4 (2–6) days.

Thus, the daily NO_X emission amount $P_{\rm day}$ is

$$\begin{aligned} P_{\rm day} &= \frac{F\,{\rm VCD}_{\rm NO_2}}{\tau f_{\rm NO_2}} \\ &= \frac{1.5}{(4\times 0.6){\rm VCD}_{\rm NO_2}} \\ &\approx 0.63{\rm VCD}_{\rm NO_2} . \end{aligned} \tag{3}$$

Considering the range of each parameter,

$$P_{\rm day} = 0.63\alpha {\rm VCD}_{\rm NO_2} \quad \alpha \in (0.21, 2.50) . \tag{4}$$

According to Fig. 7, the slope $k = 221.99 \pm 25.71$, which indicates that the increment of tropospheric NO_2 VCDs resulting from lightning flashes is 22.20×10^{25} molecules(flashes^{-1} d). Combining with Eq. (3), we determine the production of LNO_X as 20.87 (4.66–55.5) $\times 10^{25}$ molecules (NO_X) flash^{-1}, so the NO_X production per flash is 3.25 (1.08–12.9) kg flash^{-1}. The latter is larger than the 1.4 kg flash^{-1} in Beirle et al. (2004), possibly the result of regional differences. Studies have revealed more continental thunderstorms with greater lightning peak current and energy in the Northern Hemisphere. In the Southern Hemisphere, there are more maritime thunderstorms, and the individual lightning peak current and energy is smaller than that in the Northern Hemisphere (Sun et al., 2004). The individual lightning energy is proportional to LNO_X production, so that production per flash on the Tibetan Plateau should be higher than the Australian region. In addition, the correlation coefficient of lightning and NO_2 VCDs in Beirle et al. (2004) was 0.76, but in this work it is 0.79, with smaller difference. We used OTD/LIS2.3 low-resolution lightning data, including total lightning flashes without classification of lightning flash type, to obtain an annual mean of 2.1×10^7 lightning flashes over inland China. This leads to an NO_X production by lightning of 0.07 (0.02–0.27) TgN yr^{-1} over China, which is within the range of 0.016–0.384 TgN yr^{-1} from previous estimates (Table 1). In this extrapolation method, the estimate is influenced by the values of the correction factor CF, the ratio of NO_2 to NO_X in the troposphere $f_{\rm NO_2}$, and the lifetime τ of NO_2 in Eq. (1). They all have an uncertainty range as discussed above, so an uncertainty of one order of magnitude remains in the LNO_X estimate. The estimate is 0.07 TgN yr^{-1} when the CF, $f_{\rm NO_2}$ and τ are 1.5, 0.6 and 4, respectively. Meanwhile, the minimum estimate is 0.02 TgN yr^{-1} when the three parameters are 1, 0.8 and 6, respectively, and the maximum is 0.27 TgN yr^{-1} when they are 2, 0.4 and 2, respectively.

Zhou and Qie (2002) used a flash energy of 6.7×10^9 J that was proposed by Price and Rind (1994). However, Wang et al. (1998) proved that this value is at the upper limit of individual lightning energy, which may result in a larger estimate of LNO_X in China. The LNO_X estimation of Zhou and Qie (2002) is close to the upper limit of our estimation. The estimate of Sun et al. (2004) is smaller than ours. In their theoretical calculation, they used a lightning energy per flash of 4.5×10^7 J, which was observed by OTD. This value is very small, and does not consider the influence of optical thickness on light energy and the inversion of total lightning energy from luminous energy. The estimated energy is smaller than the lightning energy itself, which might reduce LNO_X estimation for China. Moreover, in the Sun et al. (2004) estimate, there may be errors from the lack of direct observational data of tropospheric NO_X.

Wang et al. (2007) suggested that soil emissions over East China amounted to 0.85 TgN yr^{-1} for 1997–2000. In better agreement with estimates of Wang et al. (2007) for East China, Jaeglé et al. (2005) found an annual budget of about 0.40 TgN for 2000, and Zhao and Wang (2009) suggested soil emissions to be about 0.0883 TgN for July 2007. Lin (2012) presented soil emissions to be about 0.38 TgN for the year 2006 over East China. The differences derive mainly from the satellite products and methods used to separate anthropogenic and natural sources of NO_X in the individual studies. According to Jaeglé et al. (2005) and Wang et al. (2007), soil emissions may have been as large as 40%–50% of anthropogenic emissions in summer for East Asia in 2000 and for East China in 1997–2000, respectively, with significant implications for the global biogeochemical cycling of N. As discussed in sections 3 and 4, soil emissions of NO_X in Region *b* are very limited compared with lightning emissions, and the intercepts of regressions in Fig. 7 reduce the influence of other sources, enhancing the significance of the regressions. We did not subtract soil emissions of NO_X from the satellite data in the current study. This would have resulted in a slight overestimation of LNO_X production over inland China. However, it can be concluded that soil emissions account for very little in the estimated LNO_X. In future work, we should consider identifying the soil and lightning emissions.

LNO_X production is related to energy dissipation per flash and air densities. Intracloud (IC) flashes account for over half the lightning flashes. As a result, lightning channels mainly distribute in the middle and upper troposphere. The altitude of the central Tibetan Plateau is high, but LNO_X production occurs primarily in the middle and upper troposphere with limited difference from other places. In addition, on the one hand, the cloud-to-ground (CG) flash energy is large than IC flashes (Price et al., 1997); while on the other hand, the ratio of IC to CG decreases with latitude (Prentice and Mackerras, 1977). The lightning data from OTD/LIS comprise total lightning flashes. The latitude of Region b belongs to central China; therefore, the effects of the increased ratio of IC to CG where the latitude is lower than Region b and the decreased ratio of IC to CG where the latitude is higher than in Region b, offset one another over China. So, the extrapolation of LNO_X from Tibet to the whole of China remains stable to some extent.

It can also be seen from previous studies that lightning activity over the Tibetan Plateau is different from other regions in terms of its weak intensity (Qie et al., 2003) and very high percentage of IC flashes occurring either within the upper dipole or more frequently within the lower dipole (Qie et al., 2005; Qie et al., 2009). This difference may result in a smaller estimate based on the relationship between NO_X production and per flash on the Plateau, because the CG flash energy is larger than that of IC flashes.

6. Conclusions

The primary goal of the present study was to analyze the spatial and temporal distributions of lightning and tropospheric NO_2 VCDs, and estimate the production of tropospheric NO_2 in China. In this analysis, the seasonal variability of the tropospheric NO_2 VCDs showed a large difference between the eastern and western regions. NO_2 density in the east was an order of magnitude larger than that in the west during summer, and two orders of magnitude in winter. In the east, the composition of tropospheric NO_2 was very complex, mainly composed of anthropogenic emissions; the lightning contribution was very small. The monthly change in tropospheric NO_2 VCDs was nearly opposite to the tendency of lightning flashes. In the western region, lightning activity and tropospheric NO_2 VCDs were strongly associated. Lightning was the main source of tropospheric NO_2 there, although lightning flashes were less frequent than in the eastern region. The effect of human activities was very weak.

On the Tibetan Plateau, tropospheric NO_X mainly comes from natural emissions, and NO_X contributions of such emissions other than lightning are very slight. The plateau is an ideal area to study the relationship between lightning and tropospheric NO_2 VCDs, because it eliminates the influence of other sources. Based on the correlation between lightning flashes and NO_2 VCDs for the plateau, LNO_X production in China is estimated as 0.07 (0.02–0.27) TgN yr^{-1} for 1997–2012, which is within the range of 0.016–0.384 TgN yr^{-1} from previous estimates.

Because of the lack of ground observation data, we still cannot entirely eliminate the effects of other sources, although they are individually very small. The monthly average data used herein are effective for depicting the seasonal variation and interannual tendencies from a macroscopic point of view, but they cannot be used to study individual thunderstorms because of the instantaneous nature of lightning. Furthermore, the influence of atmospheric circulation may change the density of NO_2 in the troposphere, which affects the correlation with lightning. In the future, it would be valuable to also use daily data for analyzing and comparing NO_X density before and after lightning occurrence in the troposphere. Additionally, atmospheric chemistry models should be used to assess various NO_X sources for improved estimation. Finally, real-time observation should be used to validate and improve estimation methods and enhance recognition of the important role of lightning in climate change in China.

Acknowledgements. This research was supported by the National Natural Science Foundation of China (Grant Nos. 91537209，91644224), the National Key Basic Research Program of China (Grant No. 2014CB441403), and the Basic Research Fund of the Chinese Academy of Meteorological Sciences (Grant No. 2016Z002). We acknowledge the free use of tropospheric NO_2 column data from www.temis.nl and lightning data from https://ghrc.nsstc.nasa.gov.

REFERENCES

Beirle, S., U. Platt, M. Wenig, and T. Wagner, 2004: NO_x production by lightning estimated with GOME. *Advances in Space Research*, **34**, 793–797.

Boccippio, D. J., and Coauthors, 2000: The Optical Transient Detector (OTD): Instrument characteristics and cross-sensor validation. *J. Atmos. Oceanic Technol.*, **17**(4), 441–458.

Boersma, K. F., H. J. Eskes, and E. J. Brinksma, 2004: Error analysis for tropospheric NO_2 retrieval from space. *J. Geophys. Res.*, **109**, D04311, doi: 10.1029/2003JD003962.

Boersma, K. F., H. J. Eskes, E. W. Meijer, and H. M. Kelder, 2005: Estimates of lightning NO_x production from GOME satellite observations. *Atmos. Chem. Phys.*, **5**, 2311–2331.

Cecil, D. J., D. E. Buechler, and R. J. Blakeslee, 2014: Gridded lightning climatology from TRMM-LIS and OTD: Dataset description. *Atmos. Res.*, **135–136**, 404–414.

Cooray, V., M. Rahman, and V. Rakov, 2009: On the NO_x production by laboratory electrical discharges and lightning. *Journal of Atmospheric and Solar-Terrestrial Physics*, **71**, 1877–1889.

Crutzen, P. J., 1970: The influence of nitrogen oxides on atmospheric ozone content. *Quart. J. Roy. Meteor. Soc.*, **96**, 320–325.

Huntrieser, H., H. Schlager, C. Feigl, and H. Höller, 1998: Transport and production of NO_x in electrified thunderstorms: Survey of previous studies and new observations at mudlatitudes. *J. Geophys. Res.*, **103**(D21), 28 247–28 264.

Jaeglé, L., L. Steinberger, R. V. Martin, and K. Chance, 2005: Global partitioning of NO_x sources using satellite observations: Relative roles of fossil fuel combustion, biomass burning and soil emissions. *Faraday Discussions*, **130**, 407–423, doi: 10.1039/b502128f.

Kang, S. C., and Z. Y. Cong, 2006: Progress in study on precipitation and aerosol chemistry in the Tibetan Plateau. *Journal of Glaciology and Geocryology*, **28**(3), 371–379. (in Chinese)

Levy, H. II, W. J. Moxim, and P. S. Kasibhatla, 1996: A global three-dimensional time-dependent lightning source of tropospheric NO_x. *J. Geophys. Res.*, **101**, 22 911–22 922.

Lin, J.-T., 2012: Satellite constraint for emissions of nitrogen oxides from anthropogenic, lightning and soil sources over East China on a high-resolution grid. *Atmos. Chem. Phys.*, **12**, 2881–2898.

Lin, Z. Y., and X. D. Wu, 1981: Climatic regionalization of the Qinghai-Xizang Plateau. *Acta Geographica Sinica*, **36**(1), 22–32. (in Chinese)

Martin, R. V., and Coauthors, 2002: Interpretation of TOMS observations of tropical tropospheric ozone with a global model and in situ observations. *J. Geophys. Res.*, **107**(D18), ACH 4-1–ACH 4-27.

Martin, R. V., B. Sauvage, I. Folkins, C. E. Sioris, C. Boone, P. Bernath, and J. Ziemke, 2007: Space-based constraints on the production of nitric oxide by lightning. *J. Geophys. Res.*, **112**, D09309, doi: 10.1029/2006JD007831.

Miyazaki, K., H. J. Eskes, K. Sudo, and C. Zhang, 2014: Global lightning NO_x production estimated by an assimilation of multiple satellite data sets. *Atmos. Chem. Phys.*, **14**, 3277–3305, doi: 10.5194/acp-14-3277-2014.

National Bureau of Statistics of China, 2012: *China Statistical Yearbook 2012*. China Statistics Press, Beijing, China. (in Chinese)

Prentice, S. A., and D. Mackerras, 1977: The ratio of cloud to cloud-ground lightning flashes in thunderstorms. *J. Appl. Meteor.*, **16**, 545–550.

Price, C., and D. Rind, 1994: Possible implications of global climate change on global lightning distributions and frequencies. *J. Geophys. Res.*, **99**, 10 823–10 831.

Price, C., J. Penner, and M. Prather, 1997: NO_x from lightning: 1. Global distribution based on lightning physics. *J. Geophys. Res.*, **102**(D5), 5929–5941.

Qian, Z. A., T. W. Wu, and X. Y. Liang, 2001: Feature of mean vertical circulation over the Qinghai-Xizang Plateau and its neighborhood. *Chinese Journal of Atmospheric Sciences*, **25**(4), 444–454. (in Chinese)

Qie, X. S., R. Toumi, and T. Yuan, 2003: Lightning activities on the Tibetan Plateau as observed by the lightning imaging sensor. *J. Geophys. Res.*, **108**(D17), 4551, doi: 10.1029/2002JD003304.

Qie, X. S., T. L. Zhang, C. P. Chen, G. S. Zhang, T. Zhang, and W. Z. Wei, 2005: The lower positive charge center and its effect on lightning discharges on the Tibetan Plateau. *Geophys. Res. Lett.*, **32**, L05814, doi: 10.1029/2004GL022162.

Qie, X. S., T. L. Zhang, G. S. Zhang, T. Zhang, and X. Z. Kong, 2009: Electrical characteristics of thunderstorms in different plateau regions of China. *Atmos. Res.*, **91**(2–4), 244–249.

Qie, X. S., and Coauthors, 2015: A review of atmospheric electricity research in China. *Adv. Atmos. Sci.*, **32**(2), 169–191. doi: 10.1007/s00376-014-0003-z

Richter, A., J. P. Burrows, H. Nüß, C. Granier, and U. Niemeier, 2005: Increase in tropospheric nitrogen dioxide over China observed from space. *Nature*, **437**, 129–132.

Schumann, U., and H. Huntrieser, 2007: The global lightning-induced nitrogen oxides source. *Atmos. Chem. Phys.*, **7**(14), 3823–3907.

Schumann, U., and Coauthors, 2000: Pollution from aircraft emissions in the North Atlantic flight corridor: Overview on the POLINAT projects. *J. Geophys. Res.*, **105**, 3605–3631.

Seinfeld, J. H., and S. N. Pandis, 2016: *Atmospheric Chemistry and Physics: From Air Pollution to Climate*. 3rd ed., Wiley, 1152 pp.

Shi, Y., Y.-F. Xia, B.-H. Lu, N. Liu, L. Zhang, S.-J. Li, and W. Li, 2014: Emission inventory and trends of NO_x for China, 2000–2020. *Journal of Zhejiang University SCIENCE A*, **15**(6), 454–464.

Sun, A. P., J. Du, Y. J. Zhang, and M. H. Yan, 2004: Calculation of global characteristics of NO_x produced by lightning. *Plateau Meteorology*, **23**(4), 481–487. (in Chinese)

Vinken, G. C. M., K. F. Boersma, J. D. Maasakkers, M. Adon, and R. V. Martin, 2014: Worldwide biogenic soil NO_x emissions inferred from OMI NO_2 observations. *Atmos. Chem. Phys.*, **14**, 10 363–10 381, doi: 10.5194/acp-14-10363-2014.

Wang, F., W. L. Lin, J. X. Wang, and T. Zhu, 2011: NO_x release from snow and ice covered surface in polar regions and the Tibetan Plateau. *Advances in Climate Change Research*, **2**, 141–148.

Wang, Y., A. W. DeSilva, G. C. Goldenbaum, and R. R. Dickerson, 1998: Nitric oxide production by simulated lightning: Dependence on current, energy, and pressure. *J. Geophys. Res.*, **103**(D15), 19 149–19 159.

Wang, Y., M. B. McElroy, R. V. Martin, D. G. Streets, Q. Zhang, and T.-M. Fu, 2007: Seasonal variability of NOx emissions over east China constrained by satellite observations: Implications for combustion and microbial sources, *J. Geophys. Res.*, **112**, D06301, doi: 10.1029/2006JD007538.

Williams, E. R., 2005: Lightning and climate: A review. *Atmos. Res.*, **76**(1–4), 272–287.

Wu, S. L., L. J. Mickley, D. J. Jacob, J. A. Logan, R. M. Yantosca, and D. Rind, 2007: Why are there large differences between models in global budgets of tropospheric ozone. *J. Geophys. Res.*, **112**, D05302, doi: 10.1029/2006JD007801.

Xiao, Z. Y., H. Jiang, and M. M. Cheng, 2011: Characteristics of atmospheric NO_2 over China using OMI remote sensing data. *Acta Scientiae Circumstantiae*, **31**(10), 2080–2090. (in Chinese)

Xu, Y. F., Y. Huang, and Y. C. Li, 2012: Summary of recent climate change studies on the carbon and nitrogen cycles in the terrestrial ecosystem and ocean in China. *Adv. Atmos. Sci.*, **29**(5), 1027–1047, doi: 10.1007/s00376-012-1206-9.

Yienger, J. J., and H. Levy II, 1995: Empirical model of global soil-biogenic NO_x emissions. *J. Geophys. Res.*, **100**, 11 447–11 464.

Yuan, T., and X. S. Qie, 2004: Spatial and temporal distributions of lightning activities in China from satellite observation. *Plateau Meteorology*, **23**(4), 488–494. (in Chinese)

Zel'dovich, Y. B., and Y. P. Raizer, 1967: *Physics of Shock*

Waves and High-Temperature Hydrodynamic Phenomena. Academic Press, San Diego, 566–571.

Zhang, X. Y., P. Zang, Y. Zhang, X. J. Li, and H. Qiu, 2007: The trend, seasonal cycle, and sources of tropospheric NO2 over China during 1997–2006 based on satellite measurement. *Science in China Series D: Earth Sciences*, **50**(12), 1877–1884.

Zhao, C., and Y. H. Wang, 2009: Assimilated inversion of NO_x emissions over East Asia using OMI NO_2 column measurements. *Geophys. Res. Lett.*, **36**, L06805, doi: 10.1029/2008gl037123.

Zhou, Y. J., and X. S. Qie, 2002: Mechanism and estimation of lightning-generated NO_x in Chinese inland area. *Plateau Meteorology*, **21**(5), 501–508. (in Chinese)

Ziereis, H., H. Schlager, P. Schulte, P F J Van Velthoven, and F. Slemr, 2000: Distributions of NO, NO_x, and NO_y in the upper troposphere and lower stratosphere between 28° and 61°N during POLINAT 2. *J. Geophys. Res.*, **105**(D3), 3653–3664.